ACS NANO
Cite This: ACS Nano 2018, 12, 11366–11375
www.acsnano.org

ARTICLE

Energetic Performance of Optically Activated Aluminum/Graphene Oxide Composites

Yue Jiang,[†,‡,¶] Sili Deng,[†,§,¶] Sungwook Hong,[∥,¶] Jiheng Zhao,[†] Sidi Huang,[†] Chi-Chin Wu,[⊥] Jennifer L. Gottfried,[⊥] Ken-ichi Nomura,[∥] Ying Li,[#] Subodh Tiwari,[∥] Rajiv K. Kalia,[∥] Priya Vashishta,[∥] Aiichiro Nakano,[∥] and Xiaolin Zheng*[,†]

[†]Department of Mechanical Engineering and [‡]Department of Materials Science and Engineering, Stanford University, Stanford, California 94305, United States

[§]Department of Mechanical Engineering, Massachusetts Institute of Technology, Cambridge, Massachusetts 02139, United States

[∥]Collaboratory for Advanced Computing and Simulations, Department of Physics & Astronomy, Department of Computer Science, Department of Chemical Engineering & Materials Science, and Department of Biological Sciences, University of Southern California, Los Angeles, California 90089, United States

[⊥]Weapons and Materials Research Directorate, U.S. Army Research Laboratory, Aberdeen Proving Ground, Aberdeen, Maryland 21005, United States

[#]Computational Science Division and Leadership Computing Facility, Argonne National Laboratory, Argonne, Illinois 60439, United States

Supporting Information

ABSTRACT: **Optical ignition of solid energetic materials, which can rapidly release heat, gas, and thrust, is still challenging due to the limited light absorption and high ignition energy of typical energetic materials (*e.g.*, aluminum, Al). Here, we demonstrated that the optical ignition and combustion properties of micron-sized Al particles were greatly enhanced by adding only 20 wt % of graphene oxide (GO). These enhancements are attributed to the optically activated disproportionation and oxidation reactions of GO, which release heat to initiate the oxidization of Al by air and generate gaseous products to reduce the agglomeration of the composites and promote the pressure rise during combustion. More importantly, compared to conventional additives such as metal oxides nanoparticles (*e.g.*, WO_3 and Bi_2O_3), GO has much lower density and therefore could improve energetic properties without sacrificing Al content. The results from Xe flash ignition and laser-based excitation experiments demonstrate that GO is an efficient additive to improve the energetic performance of micron-sized Al particles, enabling micron-sized Al to be ignited by optical activation and promoting the combustion of Al in air.**

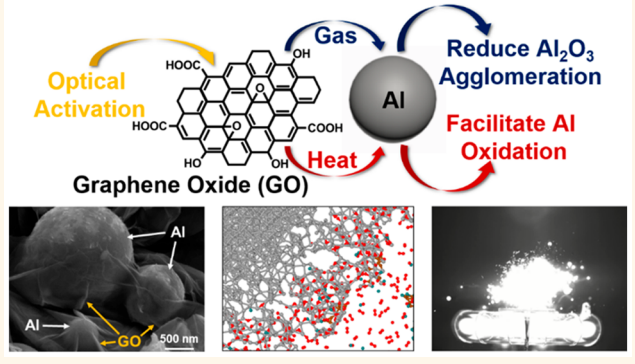

KEYWORDS: *energetic materials, aluminum, graphene oxide, flash ignition, combustion*

Aluminum (Al), with high specific energy density (31 kJ/g) and earth abundance, is a widely used fuel in solid energetic materials to generate heat, gas, and thrust for applications ranging from space propulsion and pyrotechnics to microelectromechanical systems (MEMS).[1−3] Al-based energetic materials are typically ignited at a single point by a hotwire, flame, or spark. Recently, Al particles were optically ignited by a Xe flash tube, with ignition occurring across the illuminated area.[4,5] In comparison to point ignition, areal ignition increases the heat release rate of Al. In addition, optical Xe flash ignition provides high heating rates, potentially changing the reaction dynamics of Al.[4] So far, optical Xe flash ignition has been achieved mainly for nanosized Al (n-Al)[4,6] because n-Al has lower ignition temperature and therefore is easy to ignite and burn.[7] However, the application of n-Al is limited due to the concerns of high cost, safety issues, a large portion of dead mass, and the tendency to agglomerate.[8,9] On the contrary, micron-sized Al (μ-Al) particles are widely used in practical applications, but they cannot be ignited by a low-energy Xe flash due to poor light absorption properties and high ignition temperature. Recently, optical Xe flash ignition of μ-Al particles was realized by adding WO_3 nanoparticles

Received: August 15, 2018
Accepted: October 15, 2018
Published: October 15, 2018

DOI: 10.1021/acsnano.8b06217
ACS Nano 2018, 12, 11366–11375

(diameter: 80 nm), which enhances the light absorption of μ-Al composites and provides additional oxygen to oxidize μ-Al.[10] Nevertheless, such an enhancement requires the addition of a large mass percentage of WO_3 nanoparticles (~60−80 wt %), which acts as a dead mass and hence reduces the energy density of μ-Al composites.[10] Therefore, it is of interest to enable the optical Xe flash ignition of μ-Al particles without adding much dead mass.

Graphene oxide (GO), in comparison to metal oxides (*e.g.*, WO_3), is a more attractive additive to facilitate the optical ignition of μ-Al particles. GO provides multiple benefits to optical excitation of μ-Al particles, including the enhancement of optical absorption and heat release to facilitate Al oxidation, as well as the generation of gaseous products to reduce the agglomeration of combustion products such as Al_2O_3 (Figure 1a).[11] First, the density of GO is ~1.8 g/cm^3, which is much

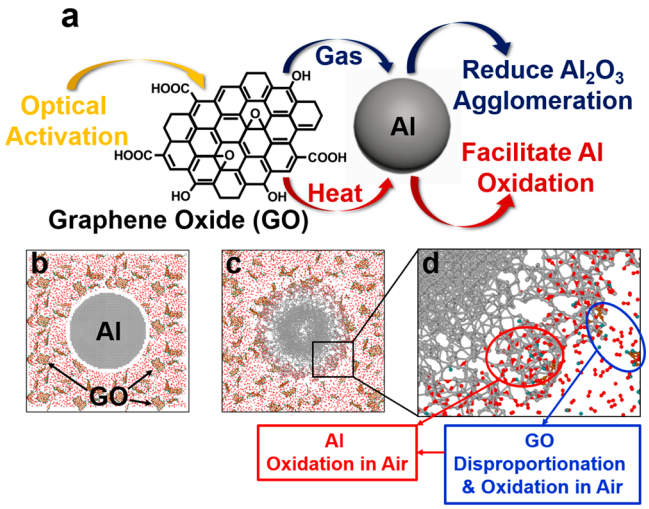

Figure 1. (a) Schematics of the Al/GO composites and the proposed mechanisms of enhancing the ignition and combustion properties of Al by GO; reactive molecular dynamics simulations of Al oxidation with GO; (b,c) sliced views of reactive molecular dynamics snapshots at 0.0 and 3.0 ps, respectively; (d) enlarged image of surface structure in (c) showing GO disproportionation and oxidation on the Al surface (blue circle) as well as the oxidation of Al (red circle) (gray, Al atoms; red, O atoms; brown, C atoms; cyan, H atoms).

lower than those of typical metal oxides (*e.g.*, Bi_2O_3, 8.9 g/cm^3; WO_3, 7.2 g/cm^3). This enables the μ-Al/GO composites to keep a high Al mass content and a high energy density. Second, GO can be optically excited by Xe flash and undergo exothermic disproportionation reaction,[12,13] which produces reduced GO (rGO), gaseous products (CO_2, H_2O, *etc.*), and heat.[14−17] Moreover, the produced rGO is also flammable in air, which may also provide more heat and gases (CO_2, *etc.*).[11] We expect that the heat will initiate the exothermic oxidation reaction of μ-Al with air,[18,19] which releases more heat to initiate exothermic reaction between μ-Al, rGO, and other gases. In fact, GO has been added to nitrocellulose to decrease the activation energy of optical ignition by a Nd:YAG laser and to increase its burning rate due to the increased specific surface area and light absorption of the composites.[20] Third, GO exhibits catalytic effects for nitromethane combustion by providing active sites to form and stabilize free radicals, leading to a lower ignition temperature and faster burning rate.[21] Finally, several reports have shown that adding GO or graphene to Al-based thermites either improves the dispersion of Al and interfacial contact between the Al and metal oxides or enhances the characteristics of the heterogeneous reactions, which increases the energy release and pressure generation.[22−26] These results demonstrate the promise of adding GO onto μ-Al particles for facilitating the optical ignition and improving combustion characteristics, such as heat and gas generation.

Herein, we show first our experimental investigation on the effect of GO addition on the optical Xe flash ignition and combustion properties of μ-Al particles (3.0−4.5 μm in average diameter) as a function of the mass percentage of GO. Our measurements showed that the minimum optical ignition energy of Al/GO composites was reduced by half when GO content was increased from 3 to 20 wt %. In addition, with only 20 wt % addition of GO, the Al/GO composites showed even better ignition and combustion performance than Al/Bi_2O_3 and Al/WO_3 with more than 60 wt % of metal oxides. Additionally, the promoting effect of GO on the microsecond and millisecond time scale energy release from μ-Al was also demonstrated with the laser-induced air shock from energetic materials (LASEM) technique. Moreover, our reactive molecular dynamics (RMD) simulation (Figure 1b−d) revealed that the disproportionation and oxidation of GO promote the oxidation of Al particles in air (Figure 1d). All of these results confirm that GO is an effective additive to enhance the energetic performance of Al with optical activation.

RESULTS AND DISCUSSION

Thermal Analysis of Pure GO in Air and Inert Environment. As shown in Figure S1a,b, GO undergoes disproportionation reaction at 200 °C with ~30% mass loss and ~1.3 kJ/g heat release under both air and Ar. However, in air, GO is further oxidized at 500 °C with ~40% mass loss and a large heat release of ~8.9 kJ/g (Figure S1a). Therefore, the thermal analysis confirms that GO can be initiated to release heat and gaseous products at low temperature, which will facilitate the oxidation of Al and reduce the agglomeration of Al_2O_3 (Figure 1a).

Material Characterizations of the As-Prepared Al/GO Composites and Their Postcombustion Products. The scanning electron microscopy (SEM) images in Figure 2a−f show the morphologies of the as-received μ-Al particles, as-received GO powders, as-prepared Al/GO (80/20 wt %) composites, and their postcombustion products after flash ignition in air. The as-received μ-Al particles are spherical and agglomerated (Figure 2a), whereas the as-received GO powders have a sheet-like morphology with smooth surfaces (Figure 2b). Their distinct difference in morphologies enables us to differentiate them in the as-prepared Al/GO sample shown in Figure 2c, where μ-Al particles are attached on the surface of GO with an overall good dispersion. An enlarged view in SEM shows that small pieces of GO are also wrapped around the surface of μ-Al particles (Figure 2d). Transmission electron microscopy (TEM) images reveal more detail relations between the μ-Al particles and the GO sheet. As shown in Figure 2g, the spherical large μ-Al particles tend to attach to the large GO sheet with some of the small particles either completely wrapped inside the GO sheet or partially covered by smaller GO flakes (Figure 2h). This suggests that the ultrasonic mixing method effectively breaks the Al agglomerates and forms the desirable intimate contact between

DOI: 10.1021/acsnano.8b06217
ACS Nano 2018, 12, 11366−11375

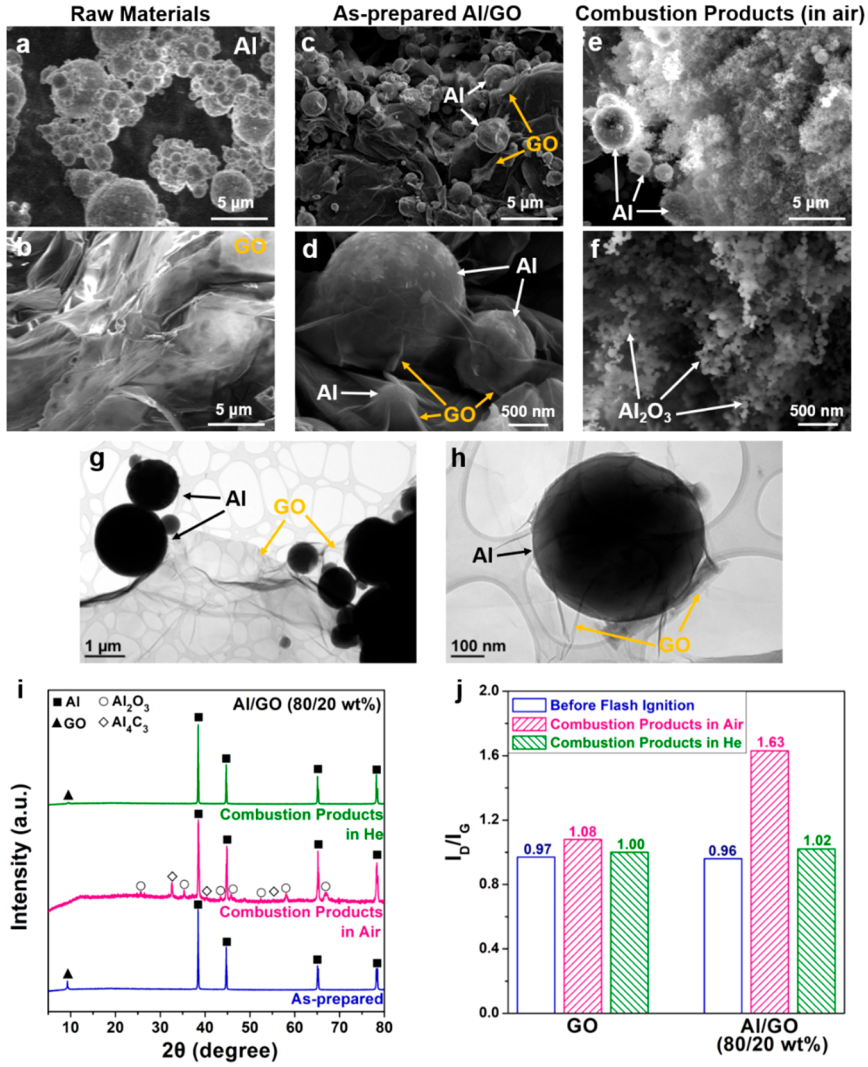

Figure 2. Morphology and composition of Al/GO (80/20 wt %) composites and postcombustion products. SEM images of (a) spherical Al particles; (b) as-received GO powders; (c) the as-prepared Al/GO composites; (d) an enlarged magnification of (c); (e) postcombustion products of Al/GO after Xe flash ignition by full power in air; and (f) enlarged magnification of (e). TEM images of (g) as-prepared Al/GO composites at 3k× magnification and (h) GO wrapping on a single Al particle at 30 k× magnification. (i) XRD results of as-prepared Al/GO (80/20 wt %) composites and its postcombustion products (in air and He). (j) I_D/I_G ratio acquired from Raman spectra of raw materials of GO, as-prepared Al/GO (80/20 wt %) composites before flash ignition and their combustion products in air and He, respectively.

GO and Al for Al oxidation. The postcombustion products of Al/GO (80/20 wt %) consist of mostly nanoparticles after full-power Xe flash ignition in air (Figure 2e,f). The nanoparticles should be mainly Al_2O_3, and this morphology is different from the products for Al ignited by conventional methods (*e.g.*, spark), which are micron-sized clusters.[27] Such a difference in the morphology of combustion products suggests the different burning behaviors of μ-Al particles from spark,[4] possibly due to a combination of areal ignition, high heating rates of flash, and the gases produced by GO disproportionation and oxidation reactions which reduce the agglomeration of Al_2O_3. Those results were also supported with energy-dispersive X-ray spectroscopy (EDXS, Figure S2) in SEM. The morphologies and elemental mapping of Al/metal oxide (Bi_2O_3 and WO_3) composites and their combustion products were further provided by SEM and EDXS (Figures S3 and S4), indicating a fair mixing in as-prepared composites and the oxidation of Al after being ignited by Xe flash.

The combustion products of Al/GO in air, according to X-ray diffraction (XRD) spectra (Figure 2i), are mainly composed of Al_2O_3 (circle symbols) and Al_4C_3 (diamond symbols). Because GO contains oxygen, we tested if GO can oxidize Al by conducting the same flash test of Al/GO in inert environment. The postcombustion products XRD spectra show peaks of Al but no peaks of Al_2O_3 and Al_4C_3 (Figure 2i), and their morphologies (Figure S5) also resemble that of the as-prepared samples (Figure 2c). The results suggest that GO is not an effective oxidizer for Al without air. In the presence of air, the heat release from GO disproportionation and oxidation reactions can initiate Al reaction with air, which is highly exothermic and promotes GO reaction with Al to Al_4C_3.[28]

The structural evolutions of GO before and after combustion in air and in He were further inspected by micro-Raman scanning microscopy. The resulting Raman spectra are plotted in Figure S6. The ratio of D-band (~1348 cm^{-1}) to G-band (~1595 cm^{-1}) (I_D/I_G ratio) is summarized in Figure 2j, and a larger ratio indicates more

DOI: 10.1021/acsnano.8b06217
ACS Nano 2018, 12, 11366−11375

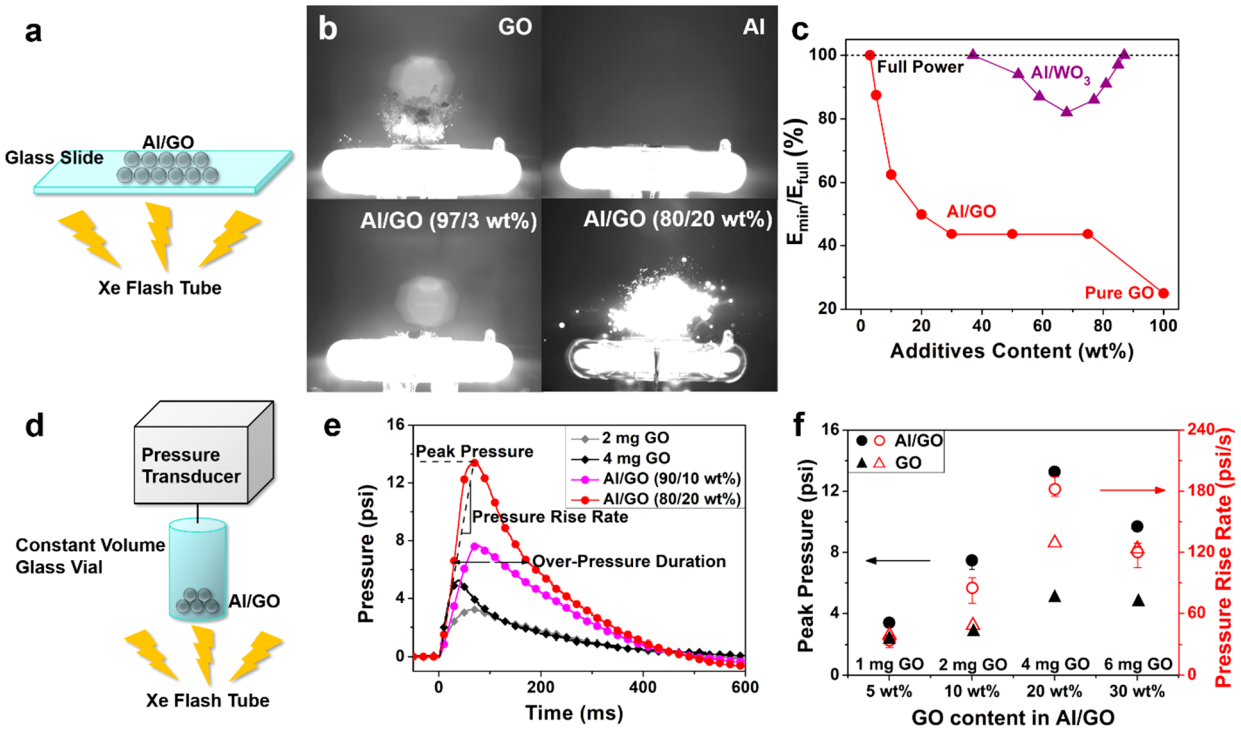

Figure 3. Measurement of the minimum ignition energy of Al/GO composites ignited by the Xe flash: (a) Schematics of the experimental setup; (b) optical images of GO, Al, Al/GO (97/3 wt %), and Al/GO (80/20 wt %) composites after being ignited by flash at full power in air; (c) normalized minimum flash ignition energy (E_{min}/E_{full}) of Al/GO composites (average Al size: 3.9 μm) in this work and Al/WO_3 from literature (average Al size: 2.3 μm) with different additive content. Measurement of the pressure−time trace of Al/GO composites ignited by the Xe flash with full power: (d) schematics of the experimental setup; (e) pressure−time traces of Al/GO (80/20 and 90/10 wt %) composites and the corresponding amount of pure GO; (f) peak pressures and pressure rise rates of Al/GO composites with different GO content.

defects in GO. First, the I_D/I_G ratio for the as-received pure GO (before flash ignition) is 0.97, which is similar to that reported in previous works about the synthesis and characterization of GO, showing a fair quality of the as-received GO.[29,30] The ratio after flash exposure is increased to 1.08 in air and 1.00 in He, suggesting that GO has undergone more structural changes in air. Second, the I_D/I_G ratio for the as-prepared Al/GO (80/20 wt %) is nearly identical to that of the as-received GO, indicating that the synthesis process does not damage the structural integrity of GO. After Xe flash ignition of Al/GO in air, the I_D/I_G ratio of GO in combustion products is significantly increased to 1.63, which is higher than that of the Al/GO before flash ignition (0.96) and combustion products of GO after being ignited in air (1.08). This suggests that GO reacts more in the presence of Al, and more defects are generated. These defects could be attributed to structural damage of rGO at high temperatures, removal of O and C on the basal plane, and reactions between C and O or Al. Finally, after being flash ignited in He, the Al/GO composites show an increment of I_D/I_G ratio (1.02) similar to that of neat GO flash ignited in He (1.00), implying that GO undergoes only disproportionation but no oxidation with flash ignition in He, as also suggested by the above thermogravimetric analysis (TGA)/differential scanning calorimetry (DSC), SEM, and XRD results.

Effect of GO Addition on the Flash Ignition of μ-Al Particles. The experimental setup of the flash ignition is illustrated in Figure 3a. For a typical experiment, 20 mg of sample was placed on a 1 mm thick glass slide on top of the Xe ring tube of a commercial flash unit (AlienBees B1600). The samples were packed to have a similar porosity of ~81−83%. The radiant energy received per unit area of Al/GO powders from the Xe flash tube, which is defined as the flash ignition energy (J/cm^2), was previously calibrated by measuring the temperature increase of a soot-covered silicon substrate exposed to the same power of flash.[31,32] Figure 3b shows the high-speed camera images of the neat GO powders, μ-Al particles, and μ-Al/GO (97/3 wt %) and μ-Al/GO (80/20 wt %) composites upon exposure to a full-power flash (2.1 J/cm^2). Under current experimental conditions, neat GO powders can react, but neat μ-Al particles cannot be ignited. With only 3 wt % of GO added into Al, we observed several sparks. When 20 wt % of GO was added to Al, the composite was ignited and burns much more violently than that of pure GO.

To quantify the effect of GO addition on the ignition of μ-Al particles, we measured the minimum flash ignition energy (E_{min}) using the same Xe flash lamp setup (Figure 3a) and the aforementioned procedures for sample preparation. Instead of using the full power (E_{full}, 2.1 J/cm^2), the power of the Xe flash lamp was gradually increased until ignition occurred, and the minimum radiant fluence was defined as the E_{min}. The effect of GO addition on E_{min} is also compared with that of WO_3 (Figure 3c) as WO_3 has been reported as an additive to reduce the E_{min} for μ-Al particles in a similar setup.[10] A normalized minimum ignition energy (E_{min}/E_{full}) is defined to compare the relative effects of GO addition as Al particles with an average size of 3.9 μm were used in our Al/GO samples, which is larger and hence harder to ignite than that of 2.3 μm Al particles that were used in Al/WO_3 composites.[10] Such a normalization also

DOI: 10.1021/acsnano.8b06217
ACS Nano 2018, 12, 11366−11375

Table 1. Comparison of Composition and Combustion Performance of Al/GO (90/10, 80/20 wt %) Composites and GO (2 and 4 mg)

sample	total mass (mg)	GO mass (mg)	Al mass (mg)	peak pressure (psi)	pressure rise rate (psi/s)	overpressure duration (ms)
Al/GO (80/20 wt %)	20	4	16	13.4	194	161
Al/GO (90/10 wt %)	20	2	18	7.7	95	190
GO (4 mg)	4	4	0	5.2	135	100
GO (2 mg)	2	2	0	3.2	52	178

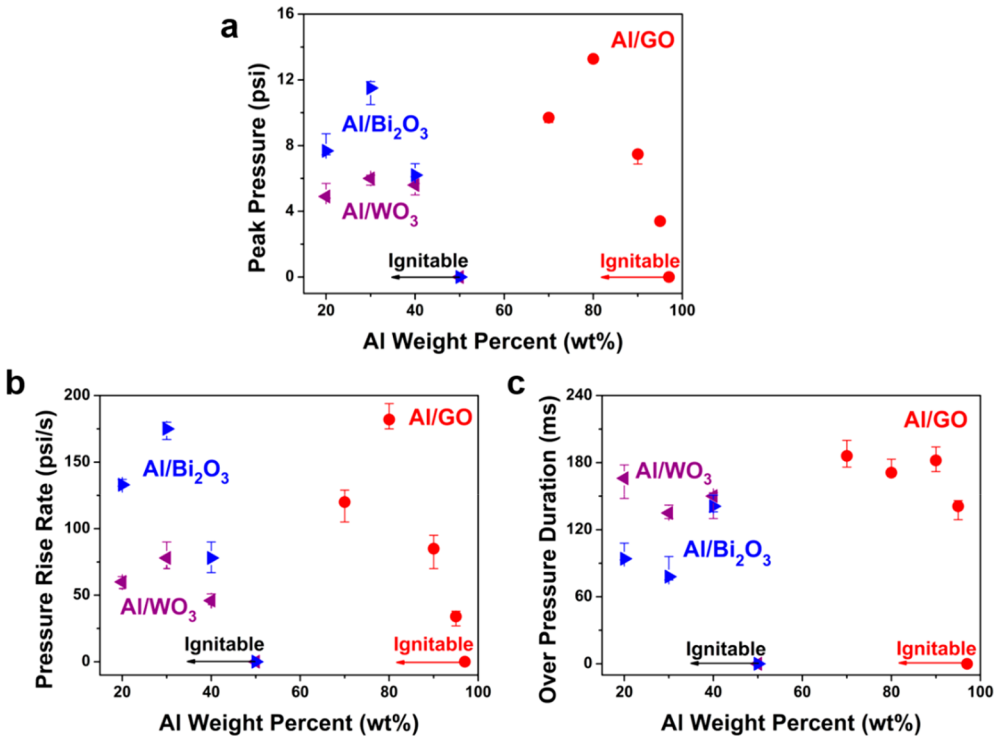

Figure 4. Comparisons of the (a) peak pressure, (b) pressure rise rates, and (c) overpressure durations of Al/GO composites and different Al/MO thermites.

avoids the uncertainty from different flash tubes and different calibration methods of the flash radiant fluence. For Al/WO_3, the ignitability limit ranges from ~37 to 87 wt % of WO_3 (80 nm) for the given full power of the flash. Within this range, E_{min}/E_{full} first decreases and then increases with increasing mass content of WO_3. The initial decrease of E_{min} comes from the enhanced light absorption and added oxidant supply from WO_3. The subsequent increase of E_{min} is due to the increased dead mass of WO_3.[10] For the optimal case, 68 wt % of WO_3 addition reduces E_{min}/E_{full} by about 18%. In comparison, the ignitability limit for Al/GO is much broader, ranging from ~3 to 100 wt % of GO. Furthermore, within this range, E_{min}/E_{full} drops sharply to ~44% with 30 wt % of GO, and it levels off with further increase of GO content. These results clearly demonstrate that GO is a much more effective additive for μ-Al particles than WO_3 nanoparticles to achieve enhanced flash ignition properties in terms of broader ignitability limits, lower minimum ignition energy, and higher Al content (lower dead mass).

Effect of GO Addition on the Pressure Evolution of the Combustion of μ-Al Particles. The combustion performance of Al/GO composites was quantified with dynamic pressure−time trace measured in a constant volume glass vial, as shown in Figure 3d. Such a test is commonly used to investigate the combustion progress of thermites.[32−35] In a typical test, 20 mg of Al/GO particles was loaded in a 20 mL glass vial, and the sample was packed into a tablet with a porosity of ~86% at the bottom of the vial. The vial initially contained ambient air and was placed on top of the Xe flash ring tube. The samples were ignited by the Xe flash lamp at full power, and the dynamic pressure and light emission from combustion were recorded by a pressure transducer (603B1, Kistler Inc.). Three tests were taken for each type of sample to determine the average and error bars showing the range of the data.

Some representative pressure−time traces are shown in Figure 3e, for which three parameters are defined to evaluate the combustion performance. The first parameter is the peak pressure, which is the maximum value of pressure recorded and is associated with the total heat release and gas generation during combustion. The second parameter is the pressure rise rate, which is the time derivative of the peak pressure and relates to the combined energy and gas release rate. The third parameter is the overpressure duration, which is the full width at half-maximum (fwhm) of the pressure peak and relates to the heat release or combustion duration.

As shown in Figure 3e, after Xe flash ignition, pure GO samples (2 and 4 mg) exhibit a rapid pressure increase due to the exothermic and gas generating disproportionation and oxidation reactions. The pressure rise became larger as the GO

DOI: 10.1021/acsnano.8b06217
ACS Nano 2018, 12, 11366−11375

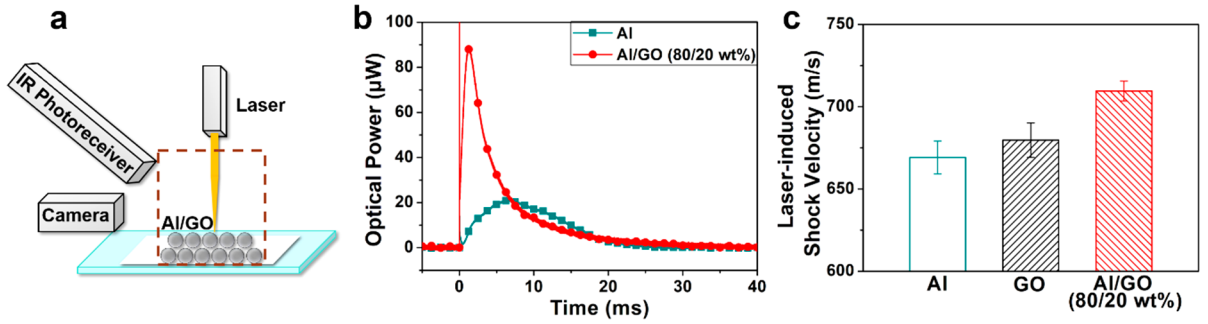

Figure 5. Measurement of the laser-induced behavior of Al/GO composites by LASEM: (a) schematics of the experimental setup, the laser-material interaction takes place in the test region of a Z-type schlieren imaging setup (dashed box); (b) time-resolved emission spectra for Al and Al/GO composites integrated over the infrared; (c) average laser-induced shock velocities for Al, GO, and Al/GO (80/20 wt %) composites.

mass loading was doubled from 2 to 4 mg. A similar trend is also observed in the Al/GO (90/10 wt % and 80/20 wt %) composites. The compositions of these four samples tested and their combustion performance are summarized in Table 1. The mass loadings (10 or 20 wt %) of the GO in the Al/GO composites are the same as those in the pure GO (2 or 4 mg) samples. For example, the Al/GO (80/20 wt %) and GO (4 mg) pressure traces show similar onset time, indicating that the disproportionation and oxidation of GO is the dominant reaction during the initial stage. Then, the Al/GO sample shows a higher peak pressure and longer overpressure duration, indicating that the oxidation of Al is triggered and becomes the main contributor to the heat release and pressure rise during the later stage. The same observation also applied to the case for the comparison between Al/GO (90/10 wt %) and GO (2 mg).

The effects of GO mass percentage in the Al/GO composites on the peak pressure (left, black symbols) and pressure rise rate (right, red symbols) are summarized in Figure 3f. The peak pressure and pressure rise rate increase with the increase of the GO content from 5 to 20 wt %; however, these metrics start to decrease when the GO content was further increased to 30 wt %. This nonmonotonic trend can be attributed to the fact that while the disproportionation and oxidation of GO are exothermic and the reactions release gases, the subsequent oxidation of Al by air is the dominant reaction for heat release. Consequently, the optimal Al/GO composites with the best combustion metrics (80/20 wt %) have the GO content that is just sufficient as a sensitizer for light absorption enhancement and initiator for Al oxidation while maintaining a relatively high Al content for large heat release. To exclude the impact of different amounts of Al in the Al/GO composites, Figure S7 shows the replotted data normalized by the mass of Al in the composites from Figure 3f. As pronounced as shown in Figure S7, the nonmonotonic trend still remains even after normalization. The results show that an optimal amount of GO addition exists for the enhancement of Al combustion performance. When the amount of GO exceeds a certain content, the agglomeration of GO and saturation of light absorption would instead limit its effect on further enhancing the ignition and combustion performance of μ-Al particles.

Comparison between of Al/GO and Al/Metal Oxide Thermites. It has been demonstrated above that GO is a better additive than WO_3 nanoparticles to enhance the flash ignition of μ-Al particles. Here, the addition of GO and metal oxides on the combustion behaviors of μ-Al particles (3.9 μm) are compared further *via* examinations of their pressure−time traces. Two typical metal oxides that are commonly used for thermites, Bi_2O_3 (80−200 nm) and WO_3 (80 nm), were chosen for this purpose. Figure 4a−c shows the comparisons of the peak pressures, pressure rise rates, and overpressure durations as a function of Al weight percentage in these mixtures. For both Bi_2O_3 and WO_3, the mixtures are ignitable only when the Al content is below 50 wt %, whereas Al/GO composites become ignitable with 97 wt % of Al. If we assume that more efficient Al combustion is represented by a larger peak pressure, larger pressure rise rate, and a longer overpressure duration, the results in Figure 4 show that a relatively much lower content of GO addition as low as ∼20 wt % instead is much more effective than high content of metal oxide additions (70 wt %). The results further emphasize the superiority of GO over metal oxides as additives in μ-Al particles to enhance the combustion performance without sacrificing the Al content.

Effect of GO Addition on the Laser-Induced Shock Velocity and Laser-Induced Combustion of μ-Al Particles. The effect of GO addition on μ-Al particles was also evaluated *via* LASEM. A simplified schematic of the LASEM setup is shown in Figure 5a. Briefly, a pulsed Nd:YAG laser (Quantel Brilliant b, 6 ns, 1064 nm, 850 mJ) is focused just below the thin residue sample surface, ablating, ionizing, and exciting the sample, thus forming a high-temperature (>10000 K) microplasma that lasts for tens of microseconds. It is important to note that the optical absorption of the sample by the laser pulse under LASEM conditions is negligible;[36] rather, the focused laser pulse serves to efficiently (at a heating rate of $\sim 10^{13}$ K/s) initiate high-temperature chemical reactions of the ablated material in the plasma. These chemical reactions are similar to those in the chemical reaction zone behind a detonation front during an explosion. The exothermic reactions of energetic materials in the laser-induced plasma region occurring within the first 10 μs can accelerate the resulting laser-induced shock wave. The expansion of the shock wave into the air above the sample is recorded with a typical Z-type schlieren imaging setup (dashed box in Figure 5a) using a high-speed color camera. The positions of the laser-induced shock waves as a function of time were measured to determine the characteristic laser-induced shock velocity of each sample. Time-resolved optical emission from the laser-induced plasma and subsequent combustion reactions were collected with an

DOI: 10.1021/acsnano.8b06217
ACS Nano 2018, 12, 11366−11375

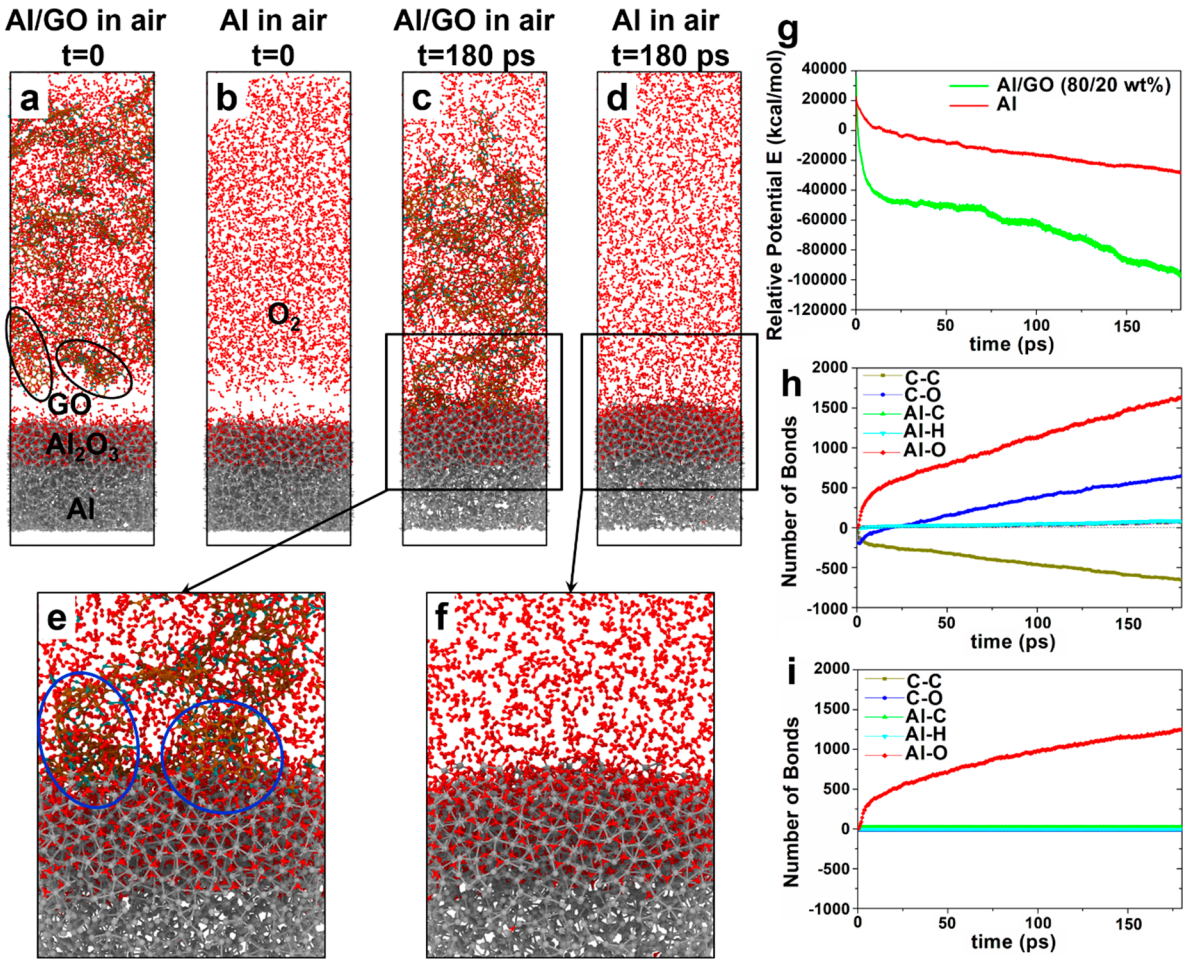

Figure 6. Initial (at 0.0 ps) snapshots of RMD simulations: (a) Al/GO (black circles indicate GO); (b) Al, final (at 180.0 ps) snapshots of RMD simulations; (c) Al/GO; (d) Al. (e,f) Enlarged images of surface structures in (c) and (d), respectively (the blue circles indicate the disproportionation and oxidation of GO on the Al surface). (g) Potential energy decreases of Al and Al/GO composites. Bond populations in (h) Al/GO composites and (i) Al as a function of simulation times. The bond populations were counted relatively with respect to the initial bond populations; *i.e.*, positive and negative values indicate increase and decrease in the bond populations, respectively, and that the numbers of each bond population indicate neighboring atom pairs.

infrared-sensitive photoreceiver. More details for the LASEM technique have been reported in previous works.[37−39]

Following the short-lived emission from the laser-induced plasma (vertical red line near t = 0 ms in Figure 5b), Al/GO (80/20 wt %) composites exhibit an optical emission much stronger than that of μ-Al, indicating an increase in the extent of the combustion reactions, as observed in the Xe flash ignition experiments. Moreover, the rate of millisecond time scale energy release is much faster for Al/GO than for μ-Al (peak combustion occurred at 1.2 and 12.7 ms, respectively), confirming that the addition of GO accelerates the oxidation of the Al during combustion reactions. As shown in images from the high-speed video (Figure S8), the GO combusts relatively rapidly (within the first few hundreds of microseconds). Al and/or AlO emission[40] from the laser-excited Al and Al/GO samples is also visible in the color video.

As the characteristic laser-induced shock velocities for inert materials are around 600 m/s,[38] the elevated shock velocities for pure Al and pure GO (Figure 5c) demonstrate that both produce some exothermic reactions on the microsecond time scale (the former through partial oxidation reactions and the latter through disproportionation reactions). The characteristic laser-induced shock velocity of the Al/GO composite is significantly higher than that of either Al or GO. The disproportionation and oxidation of GO during the laser ablation process and/or in the subsequent laser-induced plasma thus appears to accelerate the oxidation of Al on the microsecond time scale, as well, which could prove beneficial for enhancement of the detonation performance of composite energetic materials containing Al.[39,40]

RMD Simulation of μ-Al Oxidation with GO Addition. RMD simulations were conducted to explore the effects of GO on the oxidation of μ-Al in air at the molecular level. To understand the detailed reaction mechanisms of the μ-Al surface and GO/O_2 mixture, we simulated two different systems: (1) preoxidized Al slab with GO addition, *i.e.*, Al/GO (Figure 6a); (2) preoxidized Al slab without GO addition, *i.e.*, Al (Figure 6b). After 180 ps (Figure 6c,d), it was found that the oxidation of the Al slab was indeed enhanced with the presence of the GO sheets, and thus, the oxide layer became denser and thicker, in comparison with μ-Al only. Figure 6e,f further clarifies the different growths of the oxide layer in Al/GO and Al, respectively. To investigate the enhancement mechanisms, Figure 6g compares the potential energy drops of μ-Al with and without the GO addition. The potential energy of Al/GO decreased further when compared with that of pure

DOI: 10.1021/acsnano.8b06217
ACS Nano 2018, 12, 11366−11375

Al, suggesting that more heat could be released with the existence of the GO sheets during the oxidation process. Such a higher amount of heat release could be attributed to the C−C bond breaking (dark yellow curve), C−O bond formation (blue curve), and more formation of Al−O bond (red curve), as shown in Figure 6h,i. During our RMD simulation at 180 ps, the number of Al−C bonds (n = 69) was indeed negligible compared to that of Al−O bonds (n = 1716) (Figure 6h). This is because we used a preoxidized Al slab model as a reactant for reactions of Al slab and O_2 molecules with and without GO sheets. As a result, the Al slab became less reactive, leading to the formation of a smaller number of Al−C bonds during the reaction. To study the effect of different initial conditions, we also simulated the same reaction process using a bare Al slab model. During this reaction process, both Al−O and Al−C bonds were unambiguously formed, as shown in Figure S9, which could be potentially evolved toward two main products of Al_2O_3 and Al_4C_3 for long time scale RMD simulations over nanoseconds. As such, the trend in the postcombustion products from the RMD results are qualitatively consistent with our experiments (Figure 2i).

Our RMD simulations reveal the following enhancing mechanisms of GO addition. First, the intact GO undergoes disproportionation and is then attached to the Al surface. Then, O_2 molecules preferably react with the attached GO, *i.e.*, the oxidation of carbon, thus resulting in O_2 dissociation on the GO sheets. Finally, the O atoms diffuse into the subsurface of the Al slab and oxidize Al. The disproportionation of GO and its bonding to the Al surface were also confirmed by a small quantity of Al−C bond formation in the RMD snapshots in Figure 6a−f. In other words, GO exhibits the catalytic effects on the dissociation of oxygen molecules and provides a direct diffusion pathway for the dissociated O atom to reach and react with Al.

CONCLUSION

Graphene oxide has been experimentally demonstrated as an effective additive to enhance the optical ignition and combustion properties for μ-Al particles (3−4.5 μm). The results indicate that 3 wt % of GO addition is sufficient to enable the flash ignition of μ-Al particles, for which the normalized minimum ignition energy can be reduced to 44% with 30 wt % of GO addition. The results also show that 20 wt % of GO addition can optimally enhance the combustion performance after flash ignition. The Al/GO (80/20 wt %) composites are superior to the commonly used Al/nanosized metal oxide, in terms of higher Al content, lower minimum optical ignition energy, higher peak pressure, faster pressure rise, and longer overpressure duration during combustion. Similar enhancements were also observed from the microsecond and millisecond time scale energy release of Al/GO composites in LASEM experiments. The RMD simulation results further confirm that the addition of GO promotes the oxidation of μ-Al particles. The enhanced effects of GO can be attributed to the coupling heat release, catalytic effect, and gas generation. Therefore, the low molecular weight of GO can effectively advance the application of μ-Al particles as energetic materials *via* the form of Al/GO composites with the advantage of preserving higher Al content, reducing dead mass, and maintaining the high energy density.

METHODS

Synthesis of Al/GO Composites. Al/GO composites with different GO mass percentages were prepared by mechanical mixing. Mechanical mixing, also known as ultrasonic mixing, is a simple and low-cost method to prepare energetic composites.[41] Taking Al/GO (80/20 wt %) as an example, 20 mg of GO powders (99%, 0.55−1.2 nm in thickness, 0.5−3 μm in diameter, TimesNano) was sonicated in dimethylformamide (1 mg/mL) for 2 h, and 80 mg of Al particles (99.8%, 3.0−4.5 μm in diameter with an average of 3.9 μm, Alfa Aesar) was sonicated in a dimethylformamide and isopropyl alcohol solution (1:1 volume ratio, 10 mg/mL) for 15 min. Then, the two suspensions were mixed and sonicated for 1 h. The sonicated mixture was collected by filter paper (P4 grade, Fisherbrand), heated at 100 °C for 1 h to vaporize the solvent residue, and fully dried in a vacuum desiccator overnight. The same procedure was used to prepare Al/GO with other GO mass percentages and control samples of Al/metal oxide mixtures, for which we used Bi_2O_3 (80−200 nm, U.S. Research Nanomaterial Inc.) and WO_3 (80 nm, SkySpring Nanomaterials, Inc.).

Thermal Analysis of Pure GO. To investigate the disproportion and oxidation of GO, the mass change and heat flow of GO heated in both air and inert environment were investigated by TGA/DSC (Setaram Labsys Evo). For each test, 2 mg of sample powders was placed in a 100 μL alumina crucible. Samples were heated in either the air environment (40 sccm) or argon environment (40 sccm) from room temperature to 800 °C at a heating rate of 10 °C/min. For the inert environment test, the chamber was first flushed with argon (100 sccm) for 30 min to remove the residual oxygen. Before each test, the empty alumina crucible was first heated with the same process to correct the baseline of the heating process of the GO sample.

Porosity Control of Samples for Flash Ignition and Pressure Evolution Measurements. The porosity of the samples was controlled for the measurement of minimum flash ignition energy and pressure−time traces. We packed the powders in a cylindrical metal mold to control the porosity. The porosity is determined by

$$\text{porosity} = \frac{1 - (V_{Al} + V_{GO\ or\ MO})}{V_t}$$

where V_t is the total volume of the packed sample powders, and V_{Al} and $V_{GO\ or\ MO}$ are the calculated volumes from their respective mass and density.

TEM Specimen Preparation and Operations. The TEM specimens were prepared *via* a nanoparticle suspension technique by dispersing the Al/GO composites in acetonitrile onto the holey carbon film-coated TEM grid (Ted Pella). The TEM images were taken using a JEOL 2100F microscope operating at a 200 kV acceleration voltage.

RMD Simulation of Al/GO Composites. RMD simulations were performed with the reactive force field (ReaxFF).[42,43] ReaxFF parameters for Al/C/H/O elements were taken from Hong and van Duin.[44] To efficiently simulate μ-Al oxidation with GO, two different models were used: first, Al nanoparticle with O_2 and GO mixture in the simulation domain of 210.0 Å × 210.0 Å × 210.0 Å (302564 atoms) was used to confirm that our model and force field could be reasonable to describe the reactions of the Al and GO/O_2 mixture (Figure 1b−d). Then an Al slab with O_2 and GO mixture was used to efficiently simulate the reactions of μ-Al with GO in air. In our orthogonal simulation domain of 48.54 Å × 49. 47 Å × 155.0 Å, a bare Al slab model (3456 atoms) with 2500 O_2 molecules was preoxidized for 10 ps; after that, all the gas-phase species were removed, and the preoxidized Al slab was placed at the bottom of the simulation domain while the mixture of 32 GO sheets (corresponds to 20 wt %) and 2500 O_2 gas molecules were randomly distributed in the remaining vacuum layers. At the early stage of the oxidation process, the bare Al slab was too reactive to observe subtle effects of GO because the O molecules as well as GO sheets were too much preferably and simultaneously bound and dissociated on the bare Al slab. As such, we decided to use a preoxidized Al slab model, which could be less reactive when compared with the bare Al slab. The

DOI: 10.1021/acsnano.8b06217
ACS Nano 2018, 12, 11366−11375

preoxidized Al slab model was taken from our RMD trajectory of the preoxidation of the bare Al slab at 10 ps (Figure S10). The simulation domain was completely periodic in the *x*- and *y*-directions, whereas a wall boundary condition was applied to the *z*-direction. To control system temperatures during RMD simulations, the NVT ensemble with the Nose-Hoover[45,46] thermostat was applied to the entire system. A relatively small time step of 0.25 fs was used to properly capture reaction processes during RMD simulations with a temperature damping constant of 25.0 fs. During the preoxidation process, the system temperatures were kept at 2000 K. In the subsequent simulations, the preoxidized Al slab was maintained at 1500 K, whereas other gas-phase molecules were controlled at 2500 K. In doing so, we could efficiently describe the reaction of the preoxidized Al slab and GO/O_2 mixture.

ASSOCIATED CONTENT

Supporting Information

The Supporting Information is available free of charge on the ACS Publications website at DOI: 10.1021/acsnano.8b06217.

TGA/DSC of GO in air and inert environment, SEM/EDXS images of as-prepared Al/GO (80/20 wt %) composites and postcombustion products in air, SEM images of postcombustion products of Al/GO (80/20 wt %) in inert environment, Raman spectra of GO, Al/GO (80/20 wt %), postcombustion products of Al/GO (80/20 wt %) in air and He, normalized peak pressures and pressure rise rates of Al/GO composites with different GO content, snapshots from the high-speed video of the laser excitation of GO, Al, and Al/GO (80/20 wt %), potential energy evolution of bare Al as a function of RMD simulation time, and the corresponding snapshots of bare Al at 0 and 10 ps of RMD simulation (PDF)

AUTHOR INFORMATION

Corresponding Author

*E-mail: xlzheng@stanford.edu.

ORCID

Yue Jiang: 0000-0002-6017-8551
Sili Deng: 0000-0002-3421-7414
Sungwook Hong: 0000-0003-3569-7701
Jiheng Zhao: 0000-0001-8341-9031
Sidi Huang: 0000-0001-5703-0807
Ying Li: 0000-0002-0124-781X
Priya Vashishta: 0000-0003-4683-429X
Aiichiro Nakano: 0000-0003-3228-3896
Xiaolin Zheng: 0000-0002-8889-7873

Author Contributions

¶Y.J., S.D., and S.H. contributed equally to this work.

Notes

The authors declare no competing financial interest.

ACKNOWLEDGMENTS

This work was supported by Army Research Office under Agreement Number W911NF-14-1-0271 and the Office of Naval Research under Agreement Number N00014-15-1-2028. The work at USC was supported as part of the Computational Materials Sciences Program funded by the U.S. Department of Energy, Office of Science, Basic Energy Sciences, under Award Number DE-SC0014607. This research used resources of the Argonne Leadership Computing Facility, which is a DOE Office of Science User Facility supported under Contract DE-AC02-06CH11357 and the Center for High Performance Computing of the University of Southern California.

REFERENCES

(1) Brooks, K. P.; Beckstead, M. W. Dynamics of Aluminum Combustion. *J. Propul. Power* **1995**, *11*, 769−780.
(2) Wang, L. L.; Munir, Z. A.; Maximov, Y. M. Thermite Reactions: Their Utilization in the Synthesis and Processing of Materials. *J. Mater. Sci.* **1993**, *28*, 3693−3708.
(3) Rossi, C.; Zhang, K.; Esteve, D.; Alphonse, P.; Tailhades, P.; Vahlas, C. Nanoenergetic Materials for MEMS: A Review. *J. Microelectromech. Syst.* **2007**, *16*, 919−931.
(4) Ohkura, Y.; Rao, P. M.; Zheng, X. Flash Ignition of Al Nanoparticles: Mechanism and Applications. *Combust. Flame* **2011**, *158*, 2544−2548.
(5) Huang, S.; Parimi, V. S.; Deng, S.; Lingamneni, S.; Zheng, X. Facile Thermal and Optical Ignition of Silicon Nanoparticles and Micron Particles. *Nano Lett.* **2017**, *17*, 5925−5930.
(6) Yang, F.; Kang, X.; Luo, J.; Sun, L.; Xia, H.; Yi, Z.; Tang, Y. Laser Emission from Flash Ignition of Zr/Al Nanoparticles. *Opt. Express* **2017**, *25*, A932−A939.
(7) Dreizin, E. L. Metal-Based Reactive Nanomaterials. *Prog. Energy Combust. Sci.* **2009**, *35*, 141−167.
(8) Yetter, R. A.; Risha, G. A.; Son, S. F. Metal Particle Combustion and Nanotechnology. *Proc. Combust. Inst.* **2009**, *32*, 1819−1838.
(9) Sundaram, D.; Yang, V.; Yetter, R. A. Metal-Based Nanoenergetic Materials: Synthesis, Properties, and Applications. *Prog. Energy Combust. Sci.* **2017**, *61*, 293−365.
(10) Ohkura, Y.; Rao, P. M.; Sun Cho, I.; Zheng, X. Reducing Minimum Flash Ignition Energy of Al Microparticles by Addition of WO_3 Nanoparticles. *Appl. Phys. Lett.* **2013**, *102*, 043108.
(11) Krishnan, D.; Kim, F.; Luo, J.; Cruz-Silva, R.; Cote, L. J.; Jang, H. D.; Huang, J. Energetic Graphene Oxide: Challenges and Opportunities. *Nano Today* **2012**, *7*, 137−152.
(12) Gilje, S.; Dubin, S.; Badakhshan, A.; Farrar, J.; Danczyk, S. A.; Kaner, R. B. Photothermal Deoxygenation of Graphene Oxide for Patterning and Distributed Ignition Applications. *Adv. Mater.* **2010**, *22*, 419−423.
(13) Cote, L. J.; Cruz-Silva, R.; Huang, J. Flash Reduction and Patterning of Graphite Oxide and Its Polymer Composite. *J. Am. Chem. Soc.* **2009**, *131*, 11027−11032.
(14) Pei, S.; Cheng, H.-M. The Reduction of Graphene Oxide. *Carbon* **2012**, *50*, 3210−3228.
(15) Gao, W. The Chemistry of Graphene Oxide. *Graphene Oxide*; Springer: Cham, 2015; pp 61−95.
(16) Mao, S.; Pu, H.; Chen, J. Graphene Oxide and Its Reduction: Modeling and Experimental Progress. *RSC Adv.* **2012**, *2*, 2643−2662.
(17) Kim, F.; Luo, J.; Cruz-Silva, R.; Cote, J.; Sohn, K.; Huang, J. Self-Propagating Domino-like Reactions in Oxidized Graphite. *Adv. Funct. Mater.* **2010**, *20*, 2867−2873.
(18) Fan, Z.; Wang, K.; Wei, T.; Yan, J.; Song, L.; Shao, B. An Environmentally Friendly and Efficient Route for the Reduction of Graphene Oxide by Aluminum Powder. *Carbon* **2010**, *48*, 1686−1689.
(19) Wan, D.; Yang, C.; Lin, T.; Tang, Y.; Zhou, M.; Zhong, Y.; Huang, F.; Lin, J. Low-Temperature Aluminum Reduction of Graphene Oxide, Electrical Properties, Surface Wettability, and Energy Storage Applications. *ACS Nano* **2012**, *6*, 9068−9078.
(20) Zhang, X.; Hikal, W. M.; Zhang, Y.; Bhattacharia, S. K.; Li, L.; Panditrao, S.; Wang, S.; Weeks, B. L. Direct Laser Initiation and Improved Thermal Stability of Nitrocellulose/graphene Oxide Nanocomposites. *Appl. Phys. Lett.* **2013**, *102*, 141905.
(21) Sabourin, J. L.; Dabbs, D. M.; Yetter, R. A.; Dryer, F. L.; Aksay, I. A. Functionalized Graphene Sheet Colloids for Enhanced Fuel/Propellant Combustion. *ACS Nano* **2009**, *3*, 3945−3954.
(22) Thiruvengadathan, R.; Chung, S. W.; Basuray, S.; Balasubramanian, B.; Staley, C. S.; Gangopadhyay, K.; Gangopadhyay, S. A Versatile Self-Assembly Approach toward High

DOI: 10.1021/acsnano.8b06217
ACS Nano 2018, 12, 11366−11375

Performance Nanoenergetic Composite Using Functionalized Graphene. *Langmuir* **2014**, *30*, 6556−6564.
(23) Thiruvengadathan, R.; Staley, C.; Geeson, J. M.; Chung, S.; Raymond, K. E.; Gangopadhyay, K.; Gangopadhyay, S. Enhanced Combustion Characteristics of Bismuth Trioxide-Aluminum Nanocomposites Prepared through Graphene Oxide Directed Self-Assembly. *Propellants, Explos., Pyrotech.* **2015**, *40*, 729−734.
(24) Yan, N.; Qin, L.; Hao, H.; Hui, L.; Zhao, F.; Feng, H. Iron Oxide/aluminum/graphene Energetic Nanocomposites Synthesized by Atomic Layer Deposition: Enhanced Energy Release and Reduced Electrostatic Ignition Hazard. *Appl. Surf. Sci.* **2017**, *408*, 51−59.
(25) Tao, Y.; Zhang, J.; Yang, Y.; Wu, H.; Hu, L.; Dong, X.; Lu, J.; Guo, S. Metastable Intermolecular Composites of Al and CuO Nanoparticles Assembled with Graphene Quantum Dots. *RSC Adv.* **2017**, *7*, 1718−1723.
(26) Shen, J.; Qiao, Z.; Wang, J.; Yang, G.; Chen, J.; Li, Z.; Liao, X.; Wang, H.; Zachariah, M. R. Reaction Mechanism of Al-CuO Nanothermites with Addition of Multilayer Graphene. *Thermochim. Acta* **2018**, *666*, 60−65.
(27) Monk, I.; Schoenitz, M.; Jacob, R. J.; Dreizin, E. L.; Zachariah, M. R. Combustion Characteristics of Stoichiometric Al-CuO Nanocomposite Thermites Prepared by Different Methods. *Combust. Sci. Technol.* **2017**, *189*, 555−574.
(28) Chen, B.; Jia, L.; Li, S.; Imai, H.; Takahashi, M.; Kondoh, K. *In Situ* Synthesized Al_4C_3 Nanorods with Excellent Strengthening Effect in Aluminum Matrix Composites. *Adv. Eng. Mater.* **2014**, *16*, 972−975.
(29) Kim, H. J.; Lee, S.-M.; Oh, Y.-S.; Yang, Y.-H.; Lim, Y. S.; Yoon, D. H.; Lee, C.; Kim, J.-Y.; Ruoff, R. S. Unoxidized Graphene/Alumina Nanocomposite: Fracture- and Wear-Resistance Effects of Graphene on Alumina Matrix. *Sci. Rep.* **2015**, *4*, 5176.
(30) Marcano, D. C.; Kosynkin, D. V.; Berlin, J. M.; Sinitskii, A.; Sun, Z.; Slesarev, A.; Alemany, L. B.; Lu, W.; Tour, J. M. Improved Synthesis of Graphene Oxide. *ACS Nano* **2010**, *4*, 4806−4814.
(31) Aslin, H. K. Measurement of Radiant Energy Emitted by Xenon Flashlamps. *Rev. Sci. Instrum.* **1967**, *38*, 377−381.
(32) Parimi, V. S.; Huang, S.; Zheng, X. Enhancing Ignition and Combustion of Micron-Sized Aluminum by Adding Porous Silicon. *Proc. Combust. Inst.* **2017**, *36*, 2317−2324.
(33) Kim, S. B.; Kim, K. J.; Cho, M. H.; Kim, J. H.; Kim, K. T.; Kim, S. H. Micro- and Nanoscale Energetic Materials as Effective Heat Energy Sources for Enhanced Gas Generators. *ACS Appl. Mater. Interfaces* **2016**, *8*, 9405−9412.
(34) Jian, G.; Liu, L.; Zachariah, M. R. Facile Aerosol Route to Hollow CuO Spheres and Its Superior Performance as an Oxidizer in Nanoenergetic Gas Generators. *Adv. Funct. Mater.* **2013**, *23*, 1341−1346.
(35) Deng, S.; Jiang, Y.; Huang, S.; Shi, X.; Zhao, J.; Zheng, X. Tuning the Morphological, Ignition and Combustion Properties of Micron-Al/CuO Thermites through Different Synthesis Approaches. *Combust. Flame* **2018**, *195*, 303−310.
(36) Gottfried, J. Laser-Induced Air Shock from Energetic Materials (LASEM) Method for Estimating Detonation Performance: Challenges, Successes and Limitations. *AIP Conf. Proc.* **2017**, *1979*, 100014.
(37) Gottfried, J. L. Laboratory-Scale Method for Estimating Explosive Performance from Laser-Induced Shock Waves. *Propellants, Explos., Pyrotech.* **2015**, *40*, 674−681.
(38) Gottfried, J. L. Influence of Exothermic Chemical Reactions on Laser-Induced Shock Waves. *Phys. Chem. Chem. Phys.* **2014**, *16*, 21452−21466.
(39) Gottfried, J. L.; Smith, D. K.; Wu, C.-C.; Pantoya, M. L. Improving the Explosive Performance of Aluminum Nanoparticles with Aluminum Iodate Hexahydrate (AIH). *Sci. Rep.* **2018**, *8*, 8036.
(40) Gottfried, J. L.; Bukowski, E. J. Laser-Shocked Energetic Materials with Metal Additives: Evaluation of Chemistry and Detonation Performance. *Appl. Opt.* **2017**, *56*, B47−B57.
(41) He, W.; Liu, P.-J.; He, G.-Q.; Gozin, M.; Yan, Q.-L. Highly Reactive Metastable Intermixed Composites (MICs): Preparation and Characterization. *Adv. Mater.* **2018**, *30*, 1706293.
(42) van Duin, A. C. T.; Dasgupta, S.; Lorant, F.; Goddard, W. A. ReaxFF: A Reactive Force Field for Hydrocarbons. *J. Phys. Chem. A* **2001**, *105*, 9396−9409.
(43) Senftle, T. P.; Hong, S.; Islam, M. M.; Kylasa, S. B.; Zheng, Y.; Shin, Y. K.; Junkermeier, C.; Engel-Herbert, R.; Janik, M. J.; Aktulga, H. M.; Verstraelen, T.; Grama, A.; van Duin, A. C. T. The ReaxFF Reactive Force-Field: Development, Applications and Future Directions. *Npj Comput. Mater.* **2016**, *2*, 15011.
(44) Hong, S.; van Duin, A. C. T. Atomistic-Scale Analysis of Carbon Coating and Its Effect on the Oxidation of Aluminum Nanoparticles by ReaxFF-Molecular Dynamics Simulations. *J. Phys. Chem. C* **2016**, *120*, 9464−9474.
(45) Nosé, S. A Unified Formulation of the Constant Temperature Molecular Dynamics Methods. *J. Chem. Phys.* **1984**, *81*, 511−519.
(46) Hoover, W. G. Canonical Dynamics: Equilibrium Phase-Space Distributions. *Phys. Rev. A: At., Mol., Opt. Phys.* **1985**, *31*, 1695−1697.

DOI: 10.1021/acsnano.8b06217
ACS Nano 2018, 12, 11366−11375